

Structure–Property Relationship of Polymer Blends with Co-Continuous Structures Prepared by Photo-Cross-Linking

Akira Imagawa and Qui Tran-Cong*

Department of Polymer Science and Engineering, Kyoto Institute of Technology,
Matsugasaki, Sakyo-ku, Kyoto 606, Japan

Received April 24, 1995; Revised Manuscript Received September 5, 1995*

ABSTRACT: Polymer blends with co-continuous structures in the micrometer scale were obtained by photo-cross-linking of poly(2-chlorostyrene)/poly(vinyl methyl ether) (P2CS/PVME) mixtures undergoing the spinodal decomposition process. The reaction was carried out with UV light at 365 nm to induce the photodimerization of anthracenes labeled on the P2CS chains (P2CS-A). To obtain the blends with co-continuous structures of varying length scales (λ), P2CS-A/PVME blends having the same cross-link density were prepared by irradiation and subsequently annealed over different time intervals. The resulting morphology was observed by using phase-contrast optical microscopy and was analyzed by digital image analysis. It was found that the time evolution of these co-continuous structures follows the power law $\lambda \propto t^\alpha$, where α is close to 1/4. This value is smaller than 1/3, as predicted by the Lifshitz–Slyozov–Wagner law, indicating that the spinodal decomposition was slowed down by the presence of cross-links. The physical properties of these photo-cross-linked blends were examined by dynamic mechanical measurements. For the same cross-link density, the storage modulus E' of P2CS/PVME blends increases with λ , whereas the loss peaks of these co-continuous structures shift to the high temperature side. These experimental results suggest that the combination of photo-cross-linking reactions and the phase separation kinetics of polymer blends has the potential of providing a new way to design multiphase polymer materials with controllable co-continuous structures in the micrometer range.

I. Introduction

Morphology control of polymer blends has been an area of continuous interest for polymer material scientists since the past several decades, because it is expected that the physical properties such as toughness, transparency, crack resistance, etc., of multiphase polymer materials can be greatly improved by modifying their morphology.¹ So far, a wide variety of chemical and physical techniques has been exploited for these purposes. Living anionic polymerization is a popular chemical method which has been extensively utilized to control the well-defined morphology of block copolymers.² Due to the immiscibility among different polymer components in a block copolymer, microphase separation occurs in the bulk state. As a result, a number of ordered structures such as spherical domain, cylinder, or lamella is obtainable by selection of casting solvents or adjustment of molecular weights of the polymer components.³ These established chemical techniques have formed a basis for the morphology control of multiphase polymer materials in the sub-micrometer scale. However, the sizes of these ordered structures are limited in the nanometer range because it is not easy to prepare block copolymers with very high molecular weights by this technique, particularly for multicomponent block copolymers. Furthermore, the techniques, though powerful for a number of monomers, are still limited and strongly depend on the monomer reactivity. Alternatively, there are also many physical methods which have been developed to control the morphology of immiscible blends in the micrometer scale. Among them, the most popular one is the mechanical processing such as stirring or agitating the melts of immiscible polymer mixtures with an adjustable speed.⁴ These techniques have been efficiently used in practice to control the sizes, often in the micrometer range, of the

dispersed phases in incompatible polymer mixtures. In contrast to the living anionic polymerization, the highly ordered structures such as cylinder or lamella cannot be easily generated by these physical methods. For multiphase polymer materials, the correlations between morphology and mechanical properties are still not well understood, though it is generally accepted that the toughness of these materials tends to reach a maximum as the sizes of the dispersed phase approach a micrometer.¹ Therefore, it would be of great interest to develop a method to prepare multiphase polymer materials with controllable ordered structures in this particular range and subsequently characterize their physical properties.

Recently, in an effort to design such materials, we have utilized *in situ* photo-cross-linking reactions to control the morphology of binary polymer blends undergoing the spinodal decomposition process.^{5,6} It was demonstrated that the spinodal decomposition process can be efficiently frozen at different stages by taking advantage of the photodimerization of the anthracene moieties which are chemically labeled on one polymer component of the blend.⁷ However, quantitative relations between the photo-cross-linking kinetics and the resulting morphology, as well as the physical properties such as viscoelastic properties, of these photo-cross-linked blends have not yet been elucidated in great detail. In this paper, poly(2-chlorostyrene)/poly(vinyl methyl ether) (P2CS/PVME) blends were chosen as a model system for these purposes. The advantage of this particular blend is that it possesses a lower critical solution temperature (LCST) located above the ambient temperature, facilitating the experiments. Furthermore, compared to the well-known polystyrene/poly(vinyl methyl ether) blend,⁸ the large differences in refractive index and in electron density between P2CS and PVME enable one to characterize easily the phase behavior as well as the morphology of these blends by phase-contrast optical microscopy, light scattering, and small-angle X-ray scattering (SAXS). At first, the phase behavior of anthracene-labeled P2CS/PVME blends was

* To whom correspondence should be addressed.

© Abstract published in *Advance ACS Abstracts*, November 1, 1995.

investigated using small-angle scattering (SAXS), by which the spinodal temperatures and the cloud points of these blends were simultaneously determined. Based on the phase diagram constructed from these data, P2CS/PVME blends were jumped from the one-phase into the spinodal region. The growth of the concentration fluctuations with time was subsequently frozen by the photodimerization of the anthracene moieties attached on P2CS chains. The morphology resulting from the photo-cross-linking reactions was examined by using phase-contrast optical microscopy and was then analyzed by two-dimensional fast Fourier transform (FFT). The stability of the morphology arrested by this *in situ* photo-cross-linking reaction was also examined for P2CS/PVME blends having the same cross-linking density. These results are discussed in conjunction with the cross-linking reaction kinetics monitored directly by UV absorption spectroscopy. Finally, the morphology dependence of the dynamic mechanical properties of these cross-linked blends was examined and discussed.

II. Experimental Section

(1) **Samples.** Poly(2-chlorostyrene) (P2CS) was prepared by radical polymerization of 2-chlorostyrene (Tokyo Kasei, Japan) in benzene at 60 °C over 3 days. Subsequently, the polymer was chloromethylated in neat chloromethyl methyl ether (Tokyo Kasei, Japan) with zinc chloride (Aldrich) as catalyst according to the procedure reported previously.⁹ The chloromethylated poly(2-chlorostyrene) was then reacted with the potassium salt of 9-anthracenecarboxylic acid (Aldrich, recrystallized twice in ethanol) in anhydrous dimethylformamide (Aldrich) at 65 °C over 8 h. The weight average molecular weight and the polydispersity of the anthracene-labeled P2CS (P2CS-A, $M_w = 2.1 \times 10^5$, $M_w/M_n = 1.8$) were obtained respectively from the intrinsic viscosity of toluene solutions of the polymer¹⁰ and gel permeation chromatography (GPC) with standard polystyrenes as reference. The glass transition temperature of P2CS-A is 117.3 °C. The label content of the P2CS-A was determined from the absorbance of the anthracene moieties and is approximately 1 anthracene per 150 repeating units of 2-chlorostyrene. On the other hand, poly(vinyl methyl ether) (PVME, Polymer Scientific Products, $M_w = 9.6 \times 10^4$, $M_w/M_n = 2.1$, $T_g = -26.6$ °C) was purified by using methanol as a good solvent and heptane as a poor solvent. All the P2CS-A/PVME blends used in this work were prepared by casting benzene solutions containing appropriate amounts of the two polymers. These blends were sandwiched between two glass plates with an aluminum spacer used to adjust the sample thickness. These samples were dried at 90 °C under vacuum over 2 days prior to the experiments. Only P2CS-A/PVME blends with the off-critical composition (60/40) were used in this work. Upon irradiation with UV light at 365 nm, the anthracene moieties attached to P2CS chains undergo photodimerization. The photodimers form the cross-linking junctions between P2CS-A chains, resulting in a network which traps the un-cross-linked component PVME. These cross-linking junctions are permanent unless the samples are heated to temperatures higher than 200 °C, where the anthracene photodimers thermally dissociate and are converted to anthracenes.

(2) **Instruments and Data Analysis.** The phase behavior of the blends was observed by using small-angle X-ray scattering at the Synchrotron Facilities of the National Laboratory for High Energy Physics (Tsukuba, BL-10C beam line). The details were described elsewhere.¹¹ Briefly, the incident X-ray with a wavelength of 1.488 Å selected from a 2.5 GeV storage ring was point focused at the sample by using a double-flat monochromator combined with a cylindrical mirror. The distance between the sample and the detector (a one-dimensional position-sensitive proportional counter PSPC, 512 channels) was 1.9 m. The sample, with a thickness of ca. 1 mm, was sandwiched between two Mylar thin films (PET, Teijin), each with a thickness of 5 μm. Prior to the data

analysis, the scattering intensity was corrected by subtracting the absorption of the sample and the two Mylar windows from the total intensity. The experimental temperature is controlled with a precision of ±0.5 °C. All the curve fitting was carried out using a nonlinear least squares program with regression.

In the photo-cross-linking experiments, a blend with the thickness 50 μm was at first kept in a brass heating block at 100 °C (one-phase region) for 30 min and was then quickly transferred to another block which was set at 152 °C, i.e., 2 °C above the spinodal line. After 3 min, which is the time required for the sample to achieve thermal equilibrium, the blend was irradiated with UV light at 365 nm by using a mercury-xenon lamp (500 W, Model L-2424, Hamamatsu Photonics). The average intensity at this particular wavelength is ca. 70 mW/(cm²·s). After cross-linking, the morphology of the blend was observed by using a phase-contrast optical microscope (Nikon, Model XF-NTF-21). The images were then transferred to a digital image analyzer (Pias Co., Model LA-525, Japan), where two-dimensional fast Fourier transform (FFT) was performed for structure analysis. Finally, the characteristic length scale of the morphology was obtained from the one-dimensional power spectra after smoothing the data by using the binomial smoothing algorithm.¹²

The glass transition temperatures (T_g) of the blends were measured by using a differential scanning calorimetry (Mac Science, Model 3100) with a heating rate of 5 °C/min, and the midpoint of the transition was taken as T_g of the sample. The viscoelastic properties of the photo-cross-linked blends were observed by using a rheometer (Model DVE-V4, Rheology Inc., Japan). The temperature dependence of the frequency dispersion curve was obtained by a single temperature scan of 5 °C/min. Specimens with the dimensions 18 mm × 4 mm × 0.3 mm were used as samples in these experiments.

III. Results and Discussion

(1) **Phase Behavior of P2CS-A/PVME Blends.** The X-ray scattering intensity from the P2CS-A/PVME blends increases with increasing temperature, implying the existence of a lower critical solution temperature (LCST). Namely, P2CS-A/PVME blends are miscible at ambient temperature and undergo phase separation upon heating. The scattering intensity is well expressed by the Ornstein-Zernike function:

$$S(0)/S(q) = 1 + \xi q^2 \quad (1)$$

where q , the magnitude of the scattering vector, is given by $q = (4\pi/\lambda) \sin(\theta/2)$, where θ is the scattering angle and λ is the wavelength of the incident X-ray. $S(q)$ and $S(0)$ are the scattering intensities measured at an arbitrary and the zero-scattering vector q , respectively. ξ is the correlation length corresponding to the wavelength of the concentration fluctuations given by the ratio of the slope and intercept of the Ornstein-Zernike plot (eq 1).

An example of the curve fitting using the Ornstein-Zernike equation for the scattering profiles of a P2CS-A/PVME (30/70) blend obtained at several temperatures is depicted in Figure 1. To estimate the spinodal temperature (T_s) of the blend, we assume that the critical behavior of this particular blend obeys the mean-field theory and plot $1/\xi^2$ versus $1/T$ in Figure 2, where T is the absolute temperature. The linear relationship shown in this plot justifies the validity of the mean-field theory within the temperature range of the experiments. The spinodal temperature for a given composition of the blend was then obtained by extrapolating $1/\xi^2 \rightarrow 0$.¹³ On the other hand, the cloud points corresponding to these spinodal temperatures were determined from the sudden rise of the scattering intensity with temperature at a fixed scattering vector ($q = 6.33 \times 10^{-3}$

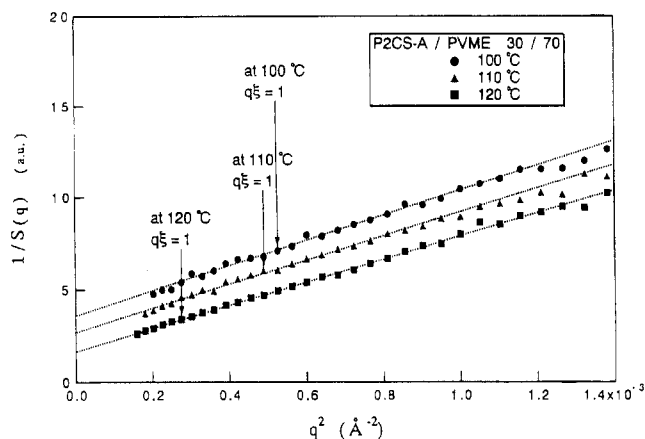


Figure 1. Ornstein-Zernike (O-Z) plots obtained at 100, 110, and 120 °C for a P2CS-A/PVME (30/70) blend. The dotted lines are the O-Z fits using eq 1.

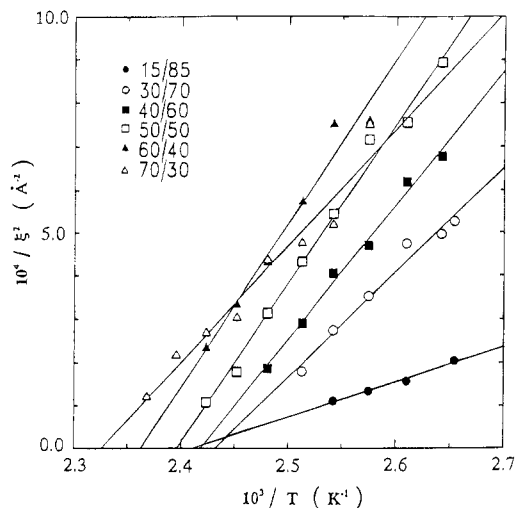


Figure 2. Temperature dependence of the correlation length ξ obtained from the O-Z equation. The spinodal temperature (T_s) was estimated by extrapolating $1/\xi^2 \rightarrow 0$.

Å^{-1}). The phase diagram constructed from these spinodal temperatures and X-ray cloud points is shown in Figure 3. The deviation of the critical point from the minimum of the coexistence curve has been previously observed in polymer blends labeled with photo-cross-linkers.⁹ An extreme case for the alteration of polymer blend miscibility by the very high label content was reported elsewhere.¹⁴

(2) Morphology Control by Photo-Cross-Linking and Structure Analysis. In order to prepare multiphase polymer materials with controllable morphology in the micrometer range, we performed *in situ* photo-cross-linking of one polymer component in a binary blend undergoing spinodal decomposition. Only P2CS-A/PVME blends with the off-critical composition (60/40) were used here. At first, a P2CS-A/PVME (60/40) blend was jumped from the one-phase (100 °C) into the spinodal region (152 °C). According to the phase diagram illustrated in Figure 3, the corresponding jump depth is 2.0 °C. After 3 min, which is the time required for the sample to reach thermal equilibrium at 152 °C, the blend was irradiated with UV light in 30 min and annealed at the same temperature over 60 min in the dark before quenched to room temperature. The glass transition temperature (T_g) of this particular composition is 31.3 °C. The T -jump diagram, the corresponding morphology, and the two-dimensional power spectra of the photo-cross-linked blend obtained under this ex-

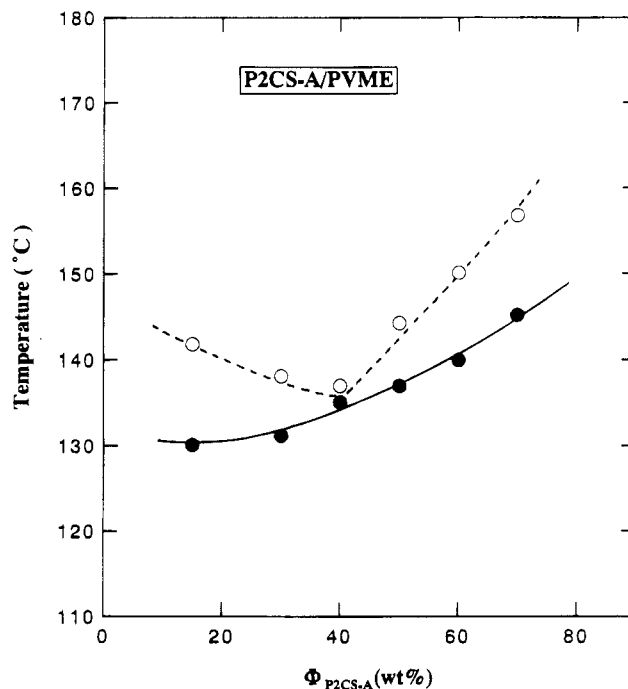


Figure 3. Phase diagram of the P2CS-A/PVME blend used in this work: (O) spinodal temperature; (●) X-ray cloud point.

perimental condition are shown in Figure 4. In contrast to this result, a P2CS-A/PVME (60/40) blend, which was jumped from 100 to 152 °C and was kept in the dark for 30 min (Figure 5a), clearly exhibits two-phase morphology, as illustrated in Figure 5b. This result indicates that the un-cross-linked blend has reached the phase equilibrium after 30 min at 152 °C. From Figure 4b, it is obvious that the co-continuous structures developing during 30 min after the T -jump were frozen by the photo-cross-linking reactions of the P2CS-A chains. This conclusion is strongly supported by the two-dimensional FFT power spectra illustrated in Figure 4c for the cross-linked blend. The above experimental results indicate that the phase separation via the spinodal decomposition process was actually arrested by the photo-cross-linking reaction of P2CS-A chains. In general, the efficiency of this freezing-in process depends on the competitions between the phase separation and the cross-linking kinetics. For a photo-cross-linked blend, the average cross-link density γ , which is defined below, can be estimated from the change in absorbance of the photo-cross-linker before and after irradiation. Namely,

$$\gamma(t) = \frac{\alpha}{2} \frac{[OD_i - OD_f(t)]}{OD_i} \quad (2)$$

where α is the label content, i.e., the average number of anthracenes covalently attached to a P2CS-A chain; OD_i is the absorbance of anthracene before irradiation; and $OD_f(t)$ is the absorbance of anthracene obtained at irradiation time t . The numerical factor 2 arises from the fact that two anthracenes photodimerize and form one cross-linking junction between two P2CS-A segments.

The dependence of γ on irradiation time obtained after correction for the cloudiness of the sample¹⁵ is shown in Figure 6. γ increases quickly with irradiation time in the first 5 min and eventually reaches an equilibrium value. Under this experimental condition, it was found that about half of the anthracenes attached to P2CS-A

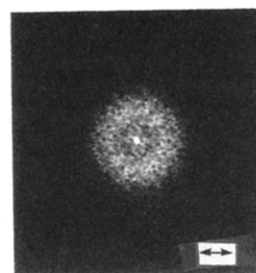
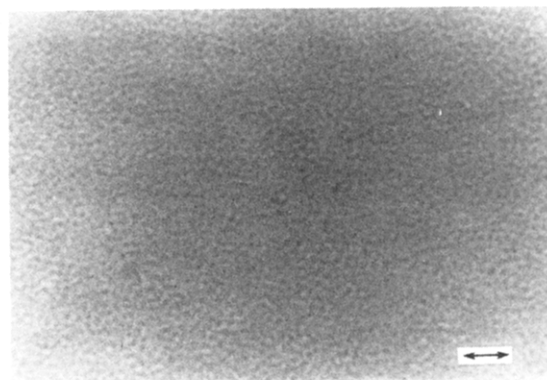
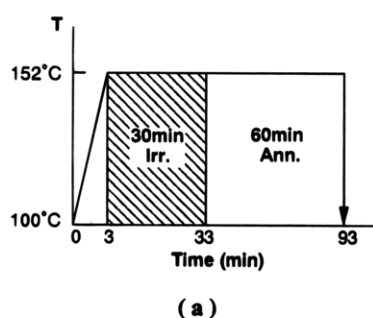


Figure 4. (a) T -jump diagram. The hatched area represents the irradiation time. "Irr." and "Ann.," respectively, stand for "irradiation" and "annealing in the dark". (b) Morphology of the P2CS-A/PVME (60/40) blend corresponding to the experimental conditions shown in (a). The scale is $5 \mu\text{m}$. (c) Two-dimensional FFT power spectra of the morphology shown in (b). The scale corresponds to $4.0 \times 10^4 \text{ cm}^{-1}$.

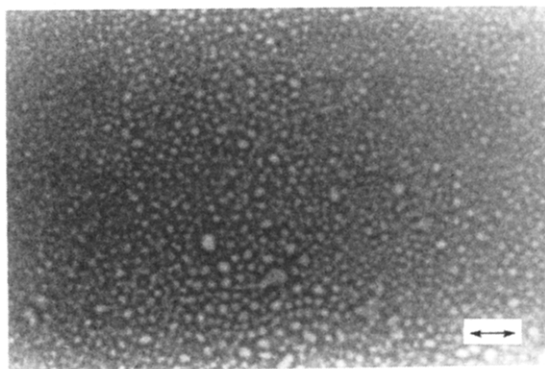
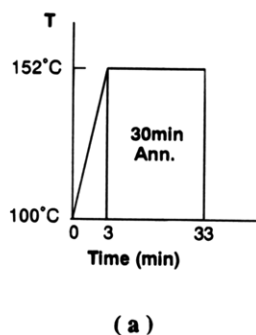


Figure 5. (a) T -jump diagram. (b) Morphology of the P2CS-A/PVME (60/40) blend corresponding to the conditions shown in (a). The scale is $5 \mu\text{m}$.

chains photodimerize after 20 min of irradiation. Therefore, the photo-cross-linked blends were actually annealed at 152°C during the last 10 min of the irradiation process. Under this condition, the average cross-link density of P2CS-A chains is 1 cross-linking junction per 300 repeating units of 2-chlorostyrene ($\gamma = 5$ junctions/chain). Since only the P2CS-A component was cross-linked, it is of great interest to examine the thermal stability of the morphology obtained under this particular condition. For this purpose, a P2CS-A/PVME (60/40) blend was irradiated at 152°C for 30 min and subsequently annealed over different time intervals in the dark. The time evolution of the morphology was monitored by using a phase-contrast optical microscope and analyzed by digital image analysis. At first, the morphology obtained after annealing was digitized and subsequently analyzed by fast Fourier transform (FFT). The characteristic length scales (λ) of the structures were obtained from the one-dimensional (1D) power

spectra extracted from the 2D FFT data. Figure 7 shows the time evolution in Fourier space of the morphology of a P2CS-A/PVME (60/40) blend annealed at 152°C after cross-linking in 30 min at the same temperature. Obviously, the maximum of the 1D power spectra shifts toward the low frequency as annealing time increases and eventually is almost unchanged after 90 min of annealing. These results imply that the morphology of the P2CS-A/PVME blend obtained just after cross-linking is not stable and relaxes upon annealing. Consequently, the phase separation kinetics of the cross-linked blend can be examined by following the annealing time dependence of the characteristic length λ of the morphology. Here, λ is the Bragg spacing given by $\lambda = 2\pi/q_{\text{max}}$ and q_{max} is the frequency corresponding to the maximum of the power spectra shown in Figure 7. The coarsening process of the morphology upon annealing was analyzed by using the power law $\lambda \propto t^\alpha$. From the plot of $\ln \lambda(t)$ versus $\ln t$, it was found

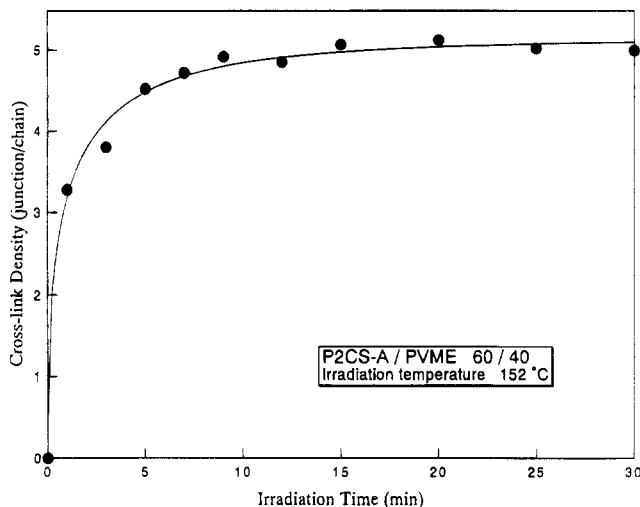


Figure 6. Photo-cross-linking kinetics of a P2CS-A/PVME (60/40) blend irradiated inside the spinodal region (152 °C) after a T -jump from 100 °C. The corresponding jump depth is 2 °C.

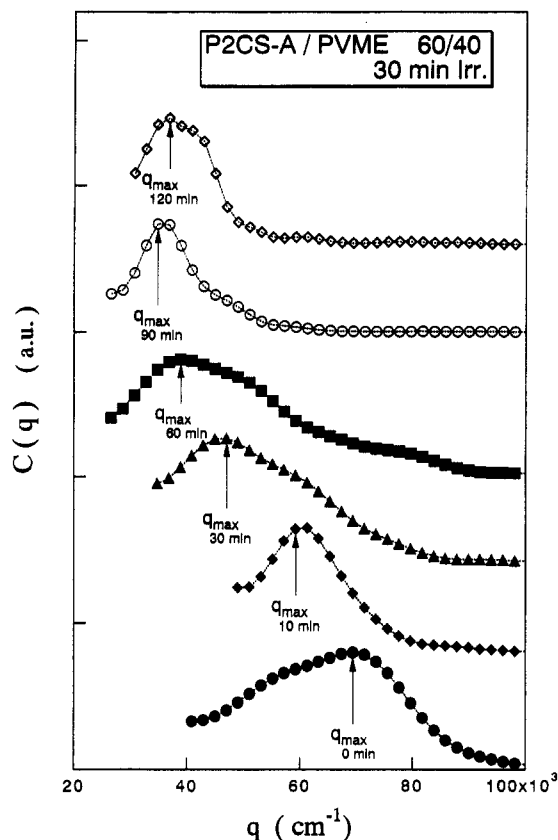


Figure 7. Morphological evolution of a photo-cross-linked P2CS-A/PVME (60/40) blend upon annealing at 152 °C. The cross-linking conditions is shown in Figure 4a. $C(q)$ is the 1D power spectrum extracted from 2D FFT data. For comparison, $C(q)$ was appropriately shifted along the ordinate. The number under each maximum indicates the annealing time.

that the most part of $\lambda(t)$ follows the above relationship with $\alpha = 1/4$. This power is smaller than the value (1/3) predicted by the Lifshitz–Slyozov–Wagner law,^{16,17} indicating that the coarsening process was slowed down by the cross-links. Recently, the effects of chemical pinning on the spinodal decomposition of binary mixtures were analyzed by using the time-dependent Ginzburg–Landau (TDGL) equation containing reaction terms.^{18,19} These authors show that α is 1/3 when the effects of the reaction are small, and α becomes 1/4 as

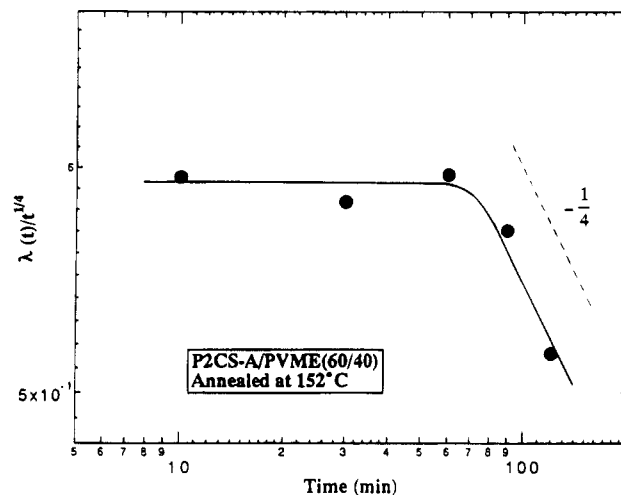


Figure 8. Coarsening kinetics of a P2CS-A/PVME (60/40) blend cross-linked at 152 °C.

the contributions of the reaction become significant. When the spinodal decomposition process is pinned by a chemical reaction, the time dependence of the characteristic length scale λ of the morphology obeys the following scaling law:

$$\lambda(t) = t^\alpha G(x) \quad (3)$$

and

$$x = kt$$

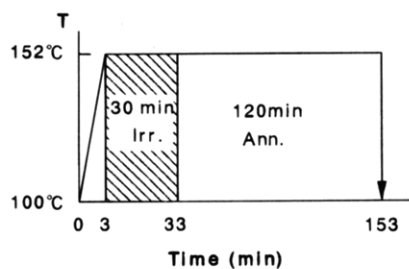
where k is the reaction rate and α is a constant.

Based on dimensional analysis, the scaling function $G(x)$ has the following features:

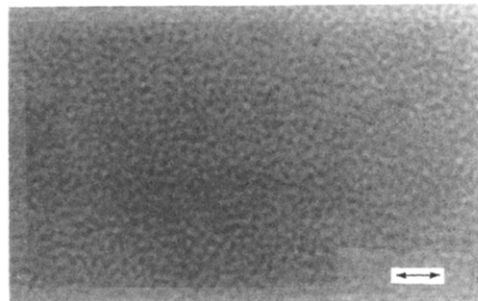
$$\begin{aligned} G(x) &= \text{constant} & \text{for } x \ll \infty \\ G(x) &\sim x^{-\alpha} & \text{for } x \rightarrow \infty \end{aligned} \quad (4)$$

In Figure 8, $G(t) = \lambda(t)/t^{1/4}$ is plotted versus annealing time t on a double logarithmic scale. Obviously, $G(t)$ does not change with time within 60 min, indicating that $\lambda(t)$ follows the $t^{1/4}$ law in this particular time range. After this period, the slope of $G(t)$ seems to asymptotically approach $(-1/4)$, implying that the spatially modulated structures of the cross-linked blend were pinned by the photo-cross-linking reaction. Furthermore, as shown in Figure 9, the structures of the cross-linked blend obtained after 120 min of annealing at 152 °C are bicontinuous. This result well corresponds to the broad peak revealed by the 2D FFT shown in Figure 7. Taking into account that (1) the structure of the cross-linked blend is co-continuous at 120 min of annealing (the longest annealing time of this experiment), (2) there are almost no changes in q_{max} with annealing time after 90 min, and (3) the analysis using the above scaling law shows the pinning of the phase separation, we can conclude that the spinodal decomposition process of the P2CS-A/PVME (60/40) blend was arrested by the reaction.

(3) Viscoelastic Properties of Binary Polymer Blends with Co-Continuous Morphology. As described above, P2CS-A/PVME blends with controllable length scales can be obtained by using photo-cross-linking reactions. The fact that these structures are stable below the glass transition temperatures of both polymers allows us to study the correlations between the physical properties and the modulated structures



(a)



(b)

Figure 9. (a) T -jump diagram. (b) Morphology of a P2CS-A/PVME (60/40) blend annealed in 120 min at 152 °C after photo-cross-linking over 30 min at the same temperature. The scale corresponds to 5 μm .

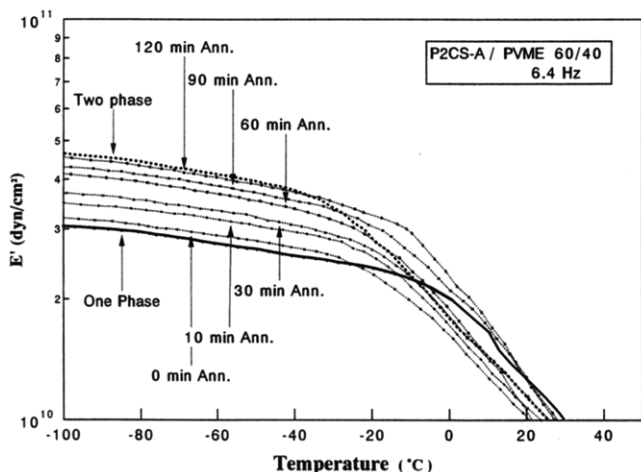


Figure 10. Temperature dependence of the storage modulus E' of the photo-cross-linked P2CS-A/PVME (60/40) blends with different characteristic length scales (λ) observed at 6.4 Hz. For comparison, E' 's of a miscible blend (solid line) and a two-phase blend (bold dotted line) are also illustrated in the same figure.

of these cross-linked blends. The viscoelastic properties of these photo-cross-linked blends were examined by dynamic mechanical measurements. At first, the cross-link densities of these samples are kept constant by irradiating the blend in 30 min with UV light, i.e., the condition shown in Figure 4a without annealing. According to the results shown in Figure 6, the average number of cross-linking junctions formed by the photodimerization of anthracenes is 5 per chain under this particular irradiation condition. The length scales of the morphology were varied by annealing the cross-linked blends in the dark over different periods of time. Figure 10 shows the temperature dependence of the storage moduli E' 's observed at 6.4 Hz for the six samples with the characteristic length scales ranging from 0.9 to 1.8 μm . For comparison, E' 's of a miscible and phase-separated P2CS-A/PVME (60/40) blends, both without cross-links, are illustrated in the same figure. At low temperatures, it seems that the magnitude of E' gradually increases with λ . However, the systematic dependence of E' on λ becomes unclear above ca. 30 °C. These results imply that the morphological changes occur in the samples and consequently affect the viscoelastic behavior of the blends. Therefore, it is reasonable to consider that the temperature dependence of E' obtained below 30 °C reflects the correlation between the storage moduli of the blends and their morphologies. For the un-cross-linked two-phase blend, the glass transition temperature (T_g) corresponding to the PVME-rich phases was observed and seems to be

lower than most of the photo-cross-linked and the one-phase blends. The higher T_g corresponding to the P2CS-rich phases could not be observed because the sample considerably deforms at high temperatures. In the past decades, there has been a number of controversial conclusions on the correlations between mechanical properties and the domain sizes of multiphase polymer materials.²⁰ Nevertheless, these results share a common feature that phase domains with a size of around few micrometers play a significant role in the mechanical properties of these materials.²¹ However, these conclusions are not clear-cut because there often exists in the sample a distribution of domain sizes or multimodal domains.²² These inhomogeneities arise from the fact that one cannot easily control the regularity of the morphology by conventional techniques such as simply adjusting the agitating or stirring rates of the mixtures. For the phase-separated materials where one polymer component is dispersed in the matrix formed by the other, it has been recognized that the stiffness of the materials decreases with increasing domain sizes.¹ This is the case of two-phase polymers where the interfaces play a key role in the mechanical properties of the materials. The photo-cross-linked P2CS-A/PVME blends obtained in this work are different from the above-mentioned multiphase polymers because P2CS-A and PVME are not completely phase separated. Namely, they do not reach the phase equilibrium because of constraints coming from the cross-linking reactions. Since the maximum length scale achievable by the experimental conditions of this work is ca. 2 μm , it is not clear that whether E' tends to reach a maximum value at a particular characteristic wavelength λ or asymptotically approaches a constant value as λ increases. On the other hand, the temperature dependence of the loss moduli E'' of a P2CS-A/PVME (60/40) blend with the two-phase structure (Figure 5b) and the blend of the same composition cross-linked for 30 min at 152 °C ($\gamma = 5$ junctions/chain) is shown in Figure 11. For comparison, E'' 's of a neat P2CS-A and a P2CS-A/PVME (60/40) blend annealed in 120 min after cross-linking are also illustrated in the same figure. Compared to the un-cross-linked blend with two-phase structures, the maximum in E'' of the blend obtained just after cross-linking (0 min of annealing) slightly shifts to the high temperature side. This is because the loss peak observed in Figure 11 for the two-phase sample corresponds to the PVME-rich phases. For the blend with the same cross-link density, the maximum of E'' shifts further to the high temperature side as the characteristic wavelength λ increases (120 min of annealing). Similar behavior was also observed for the temperature dependence of the corresponding $\tan \delta$ of

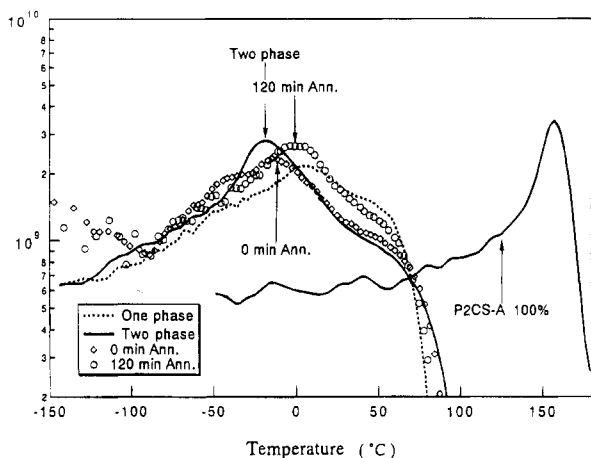


Figure 11. Temperature dependence of the loss modulus E'' of the P2CS-A/PVME (60/40) blends prepared under various conditions. "Ann." stands for annealing in the dark after photo-cross-linking over 30 min at 152 °C. The data were taken at 6.4 Hz.

these blends. The maxima of the $\tan \delta$ for the blends with the spinodal structures are located at temperatures between those of the one-phase and the two-phase samples. This feature has been previously observed by dielectric relaxation for polystyrene/poly(2-chlorostyrene) blends photo-cross-linked during the spinodal decomposition process.^{5,6} Furthermore, the $\tan \delta$ peaks of these photo-cross-linked blends are very broad, exhibiting the typical viscoelastic properties of interpenetrating polymer networks.

IV. Summary and Conclusion

We have demonstrated that photo-cross-linking of one polymer component in a binary polymer mixture undergoing spinodal decomposition process can provide a unique way to design multiphase polymer materials with controllable morphology. For poly(2-chlorostyrene)/poly(vinyl methyl ether) (P2CS/PVME) blends, the following results were obtained.

(1) With an average cross-linking density of 5 junctions/chain, the structures that developed during the spinodal decomposition process of P2CS-A/PVME blends can be frozen. Upon reheating, these co-continuous structures first grow slowly with time according to the power law $\lambda \propto t^\alpha$ with $\alpha = 1/4$ and eventually were pinned by these cross-linking junctions. The whole coarsening process can be well expressed by a scaling law developed recently for the chemical pinning of the spinodal decomposition process.

(2) Dynamic mechanical measurements of these photo-cross-linked blends seem to reveal that the dynamic modulus E' increases with the length scale of these structures. The loss peaks are located in the temperature range between those of the one-phase and two-phase samples. Furthermore, these maxima slightly

shift toward the high temperature side as the characteristic length scale increases.

Acknowledgment. Financial support from the Ministry of Education, Science and Culture, Japan (Grants-in-Aid 06651052 and 07651109), is gratefully acknowledged. The SAXS experiments in this work have been performed with the approval of the Photon Factory Program Advisory Committee, National Laboratory for High Energy Physics, Tsukuba, Japan, through Grant 93G243. We thank Sharon C. Glotzer (National Institute of Standards and Technology, NIST, MD) for useful discussions. A.I. thanks the Sekisui Chemical Co. (Osaka, Japan) for a scholarship. Finally, the technical assistance of Asuka Harada and Naoki Kawazoe (KIT) is also greatly appreciated.

References and Notes

- (1) For example, see *Rubber-Toughened Plastics*; Keith Riew, C., Ed.; Advances in Chemistry Series No. 222; American Chemical Society, Washington, DC, 1989.
- (2) For example, see Morton, M. *Anionic Polymerization: Principles and Practice*; Academic Press: New York, 1983.
- (3) Molau, G. E. *Kolloid Z. Z. Polym.* **1970**, *238*, 4931.
- (4) Echte, A. *Angew. Makromol. Chem.* **1977**, *58/59*, 175.
- (5) Tran-Cong, Q.; Nagaki, T.; Nakagawa, T.; Yano, O.; Soen, T. *Macromolecules* **1989**, *22*, 2720.
- (6) Tran-Cong, Q.; Nagaki, T.; Yano, O.; Soen, T. *Macromolecules* **1991**, *24*, 1505.
- (7) Tran-Cong, Q.; Imura, M.; Soen, T.; Shibayama, M. *Polym. Eng. Sci.* **1993**, *33*, 772.
- (8) Bank, M.; Leffingwell, J.; Thies, C. *Macromolecules* **1971**, *4*, 43.
- (9) Tran-Cong, Q.; Kawakubo, R.; Sakurai, S. *Polymer* **1994**, *35*, 1236.
- (10) Matsumura, K. *Makromol. Chem.* **1969**, *124*, 204.
- (11) Ueki, T.; Hiragi, Y.; Kataoka, M.; Inoko, Y.; Amemiya, Y.; Izumi, Y.; Tagawa, H.; Muroga, Y. *Biophys. Chem.* **1985**, *23*, 115.
- (12) Marchand, P.; Marmet, L. *Rev. Sci. Instrum.* **1983**, *54*, 1034.
- (13) Han, C. C.; Bauer, B. J.; Clark, J. C.; Muroga, Y.; Matsushita, Y.; Okada, M.; Tran-Cong, Q.; Chang, T.; Sanchez, I. C. *Polymer* **1988**, *29*, 2002.
- (14) Tamai, T.; Imagawa, A.; Tran-Cong, Q. *Macromolecules* **1994**, *27*, 7486.
- (15) The correction for the effects of the sample cloudiness was carried out by using the transmission data of the photo-cross-linked blends measured at two wavelengths. One is inside and the other is outside of the absorption range of anthracene. Kawazoe, N.; Imagawa, A.; Tran-Cong, Q. To be submitted for publication.
- (16) Lifshitz, I. M.; Slyozov, V. V. *J. Phys. Chem. Solids* **1961**, *19*, 35.
- (17) Furukawa, H. *Adv. Phys.* **1985**, *34*, 703.
- (18) Glotzer, S. C.; Coniglio, A. *Phys. Rev. Lett.* **1994**, *50*, 4241.
- (19) (a) Glotzer, S. C.; Stauffer, D.; Jan, N. *Phys. Rev. Lett.* **1994**, *72*, 4109. (b) Glotzer, S. C.; Di Marzio, E. A.; Muthukumar, M. *Phys. Rev. Lett.* **1995**, *74*, 2034.
- (20) For example, see Keskkula, H. *Optimum Rubber Particle Size in High-Impact Polystyrene: Further Considerations*, in ref 1, p 289.
- (21) Haaf, F.; Breuer, H.; Echte, A.; Schmitt, B. J.; Stabenow, J. *J. Sci. Ind. Res.* **1981**, *40*, 659.
- (22) Hobbs, S. Y. *Polym. Eng. Sci.* **1986**, *26*, 74.

MA950559X